



This is the peer reviewed version of the following article: Huang, Wan-Yi, Ya-Pei Wang, Yasser S. Mahmmod, Jun-Jie Wang, Tang-Hui Liu, Yu-Xiang Zheng, Xue Zhou, Xiu-Xiang Zhang, and Zi-Guo Yuan. 2019. "A Double-Edged Sword: Complement Component 3 In Toxoplasma Gondii Infection". PROTEOMICS, 1800271. Wiley. doi:10.1002/pmic.201800271, which has been published in final form at <https://doi.org/10.1002/pmic.201800271>. This article may be used for non-commercial purposes in accordance with Wiley Terms and Conditions for Use of Self-Archived Versions

19 **Abstract**

20 We artificially infected Sprague Dawley (SD) rats and Kunming (KM) mice with type II *Toxoplasma*
21 *gondii* (*T. gondii*) strain Prugniaud (Pru) to generate toxoplasmosis, which is a fatal disease mediated
22 by *T. gondii* invasion of the central nervous system (CNS) by unknown mechanisms. We aimed to
23 explore the mechanism of differential susceptibility of mice and rats to *T. gondii* infection. Therefore,
24 we established a strategy of isobaric tags for relative and absolute quantitation (iTRAQ) to identify
25 differentially expressed proteins (DEPs) in the rats' and the mice's brains compared to the healthy
26 groups. Complement component 3 (C3) was upregulated and the tight junction (TJ) pathway showed
27 a disorder in KM mice, which was susceptible to *T. gondii* infection. In the CNS, we presumed that
28 *T. gondii*-stimulated C3 disrupts the TJ of the blood-brain barrier (BBB). This effect allows more *T.*
29 *gondii* passing to the brain through the intercellular space.

30 **Statement of significance of the study**

31 Rat and mouse models for *T. gondii* infection are proper pathophysiological models to study the
32 toxoplasma encephalopathy, and the consequent severe mental disorders, because these two animals
33 have different susceptibility to *T. gondii* infection. To explore the reason for this difference, we
34 analyzed the cerebral proteome in rats and mice during chronic *T. gondii* infection. Interestingly, our
35 results underlined alterations of complement and coagulation cascades, and tight junction pathways
36 in the mouse brain. Specifically, we evaluated the relationship between C3 and TJ during *T. gondii*
37 infection, which supports the paracellular entry mechanism.

38 **Keywords:** Blood-brain barrier; Central nervous system; Complement component 3; *Toxoplasma*
39 *gondii*; Paracellular entry mechanism

40 **1. Introduction**

41 *Toxoplasma gondii* (*T. gondii*), a critical zoonotic parasite, infects almost all warm-blooded animals,
42 including human-beings, worldwide^[1]. The infection rates of this parasite are estimated at 30% in
43 humans, but it geographically differs from region to region^[2, 3]. Because the most severe
44 complications occur due to infection of the central nervous system (CNS)^[4], it is important to
45 elucidate how *T. gondii* transits across the blood-brain barrier (BBB) and enters into the CNS.
46 Previous studies have reported two primary mechanisms explaining how *T. gondii* goes through the
47 BBB, including Trojan-horse like mechanism and a transcellular crossing mechanism^[5, 6].

48

49 *T. gondii* invades the host cells and persists as intraneuronal cysts, resulting in damage to the CNS in
50 varying degrees, because the parasites are suppressed by the immune system but not eliminated^[7].
51 Rats and mice are widely used as experimental animals for *T. gondii* infection due to their different
52 susceptibility^[8, 9]. Specifically, adult rats have an innate resistance to *T. gondii*^[10]. Tissue infections
53 induced by cysts appeared in a subclinical form in the immunocompetent rats, though they were
54 infected with the RH strain (type I genotype)^[9]. On the other hand, mice died when infected with type
55 I genotype strains, irrespective of the infective dose^[10]. Compared to type I strains, types II and III
56 strains are less virulent to mice, and the infective doses of those strains are significantly higher for
57 rats than for mice, irrespective of the administration routes^[11]. Moreover, the *T. gondii* cysts are
58 abundantly found in the brains of mice but infrequently found in the brains of rats^[9, 12]. In agreement
59 the rat brain has lower risk of *T. gondii* infection, with no visible histological damage^[12, 13]. Compared
60 to rats, the learning capacity of mice is much more conspicuously retarded by a *T. gondii*-infection^[14].

61 However, at present, no research has been performed on this kind of difference, and the exact
62 mechanism is still poorly understood.

63

64 Our goal was to explore the mechanisms of the different susceptibility of mice and rats to *T. gondii*.

65 Comparing to control groups, we established an iTRAQ-based strategy to identify differentially
66 expressed proteins (DEPs) of infected Sprague Dawley (SD) rats and Kun Ming (KM) mice brains.

67 Afterwards, we used KEGG pathways to analyze the DEPs patterns. Interestingly, in mice brain, we
68 identified two specific pathways: the complement and coagulation cascades pathway and the tight

69 junction (TJ) pathway, related to the host immune system and the brain intrusion of *T. gondii*,

70 respectively. The two pathways contained 9 and 10 significant DEPs, among them the complement

71 component 3 (C3), whose expression was increased 11 times. We hypothesize that C3 mediates the

72 differences in this parasite-host interaction mechanism through disrupting TJ of the BBB to allow *T.*

73 *gondii* invasion of the brain. Repression of the pharmacology or genetics may reduce the damage in

74 the host, suggesting a therapeutic opportunity.

75

76 **2. Materials and Methods**

77 **2.1 Animals and Parasites**

78 The SD rats and KM mice were purchased from the Guangdong Medical Laboratory Animal Center,
79 and were bred under specific pathogen-free conditions at South China Agricultural University.

80 Parasites were harvested from the brains of KM mice that had been chronically infected with the Pru

81 strain (preserved in our laboratory), a type II strain of *T. gondii*. The brain tissue of these animals was

82 dispersed in normal saline. The final concentration of the infectious agent was adjusted to a dose of
83 10 cysts/0.2 ml for mice and a dose of 50 cysts/0.5 ml for rats ^[11, 13], which were administered orally
84 by gavage.

85

86 **2.2 Sample collection for quantitative proteomic analysis**

87 In total, 18 SPF KM mice (9 males, 9 females, 56 days old), and 9 SPF rats (4 males, 5 females, 60
88 days old) were infected with type II *T. gondii* Pru strain, and were randomly divided into 3 groups.
89 Each group contained 6 mice and 3 rats. After 30 days of infection, we collected brain tissue from
90 the infected KM mice and rats. Simultaneously, we collected brain tissue from 18 uninfected KM
91 mice and 9 uninfected rats at similar age and sex to serve as uninfected control group. Each of the
92 brain tissue samples was divided into 3 equal parts; two parts were processed for proteomics analysis
93 (one as the biological replicate, the other as the technical replicate), while the last part was used for
94 qRT-PCR validation. All animal care procedures were conducted in conformity with NIH guidelines
95 (NIH Pub. No. 85-23, revised 1996) and were approved by the Animal Ethics Committee of South
96 China Agricultural University (SCAUAEC-2015-054).

97

98 Using a mortar and pestle, 100 mg brain tissue from each animal was ground into a fine powder and
99 preserved in liquid nitrogen. Then, we used the Radio immunoprecipitation assay (RIPA) Lysis Buffer
100 (50mM Tris-HCl, 150mM NaCl, 1% SDS, 1% SDC pH 8.0, 0.1% Triton X-100) to extract total
101 proteins from each sample. The samples were sonicated (20 Watts, 10 times) and centrifuged (4°C,
102 12,000 rpm, 20 min).

103

104 **2.3 Trypsin digestion and iTRAQ labeling**

105 We used the BCA method (BCA Protein Assay Kit, Biotech) to determine the protein
106 concentrations^[15], and utilized the filter-aided sample preparation (FASP) method to digest
107 proteins^[16]. Briefly, we reduced the alkylated, and subjected it to the tryptic hydrolysis of each protein
108 sample (100 µg). iTRAQ labeling was performed according to manufacturer's protocol (Applied
109 Biosystems, Sciex). The samples of infected micewere labeled with iTRAQ tag 114 and 115, while
110 the samples of control mice were labeled with tag 113 and 116. The samples of infected rats were
111 labeled with iTRAQ tag 119 and 121, while the samples of control rats were labeled with tag 117 and
112 118. All labeled samples were pooled together and vacuum-dried.

113

114 **2.4 High-pH Reversed-Phase Chromatography**

115 We carried out a high pH Reverse Phase Fractionation (hpRP) chromatography using a Dionex
116 UltiMate 3000 high-performance Liquid Chromatography (LC) system, whose autosampler and
117 ultraviolet (UV) detection was equipped with collection option of the micro fraction. We diluted the
118 iTRAQ labeled samples in buffer A (20 mM NH₄HCO₂, pH 10) before High-Performance Liquid
119 Chromatography (HPLC) on a Gemini-NX C18 columns (3 µm, 2 × 150 mm, 110 A, Phenomenex)
120 with buffer A (mobile phase A), and buffer B (80% ACN/20% 20 mM NH₄HCO₂, mobile phase B).
121 At a flow rate of 0.2 mL/min, the peptides were eluted with a gradient of 0%–5% mobile phase B for
122 10 min, 5%–10% mobile phase B for 10 min, 15%–37% mobile phase B for 60 min, 37%–95%
123 mobile phase B for 5 min, and 95% mobile phase B for 5 min. The UV absorbance was set at 214/280

124 nm to collect fractions every 1 min for 12 fractions per each sample. The fractions were dried for
125 further analysis.

126

127 **2.5 LC-MS/MS Analysis**

128 The samples were separated by a linear gradient, which was formed by mobile phase A (0.1% FA,
129 5% ACN) and mobile phase B (0.1% FA, 80% ACN). In 40 min, the mobile phase B was changed
130 from 5% to 35% at a flow rate of 300 nL/min. We used a Triple TOF 5,600 system (AB SCIEX) with
131 an information dependent mode to perform the Mass Spectrometer (MS) analysis. Using 100 ms
132 accumulation time per spectrum, in high-resolution mode (70,000), we dynamically acquired MS
133 spectra across the mass range of 350-1,800 m/z. Up to 20 precursors per cycle was selected for
134 fragmentation from each MS spectrum, where each precursor has a minimum accumulation time of
135 120 s and a dynamic exclusion of 20 s. The high sensitivity mode (resolution: 17,500) of tandem mass
136 spectra were used, which has rolling collision energy and an iTRAQ reagent collision energy
137 adjustment.

138

139 **2.6 Protein identification and data analysis**

140 Via Proteome Discoverer 1.4 (Thermo Fisher Scientific), the raw data were converted to peak lists,
141 which are MASCOT generic format (.mgf) files. For in-depth proteome analysis and protein
142 quantitation analysis, we searched the Uniprot-mouse database and the Uniprot-rat database
143 (www.uniprot.org) with the ProteinPilot™ Software 5.0 (Applied Biosystems Sciex). This software
144 is based on Paragon Algorithm to convert the peptide analysis data into differential protein analysis

145 data (Unused > 1.3, Peptides (95%) ≥ 2). To ensure up- and downregulation authenticity, a *P-value*
146 < 0.05 and a fold change ≥ 2 (FC ≥ 2) and a FC ≤ 0.5 were used in the analysis. To understand the
147 relationships between the mice and rats infected with *T. gondii*, we used Venn diagram
148 (<http://bioinformatics.psb.ugent.be/webtools/Venn/>) and DAVID (<https://david.ncifcrf.gov>) to
149 compare the DEPs and their biological functions. KEGG database was used for biological pathway
150 analysis of these DEPs (<http://www.genome.jp/kegg/>), where every protein's name, sequence and
151 functional information are provided by UniProt Databases (<http://www.uniprot.org/>).

152

153 **2.7 Quantitative real-time PCR analysis**

154 We used quantitative real-time PCR (qRT-PCR) analysis to verify the expression of DEPs from the
155 iTRAQ analysis. Using the manufacturer's protocols of RNAiso Plus (TaKaRa, Dalian, China), total
156 RNA was extracted from the infected and control KM mice's and rats' brains. Then, we resuspended
157 the final total RNA into RNase-free water and measured its concentration and purity using the ultra-
158 microspectrophotometer (Thermo Scientific Nanodrop 2000, Waltham, MA, USA). cDNA was
159 synthesized using the SYBR PrimeScript™ RT Master Mix (Perfect Real-Time) Kit (TaKaRa, Dalian,
160 China). Gene-specific primers for qRT-PCR were designed with Premier 5.0 software (Premier
161 Biosoft International, Palo Alto, CA, USA). According to the manufacturer's instructions (TaKaRa
162 Dalian, China), qRT-PCR was performed on a Rotor-Gene Q (Qiagen) real-time system with SYBR
163 Green master mix (SYBR Premix Ex Tag TMII; TaKaRa Bio; <http://www.TaKaRa-bio.com>). The
164 thermal profile of qRT-PCR was 5 min at 95°C followed by 40 cycles of 30 s at 95°C and 1 min at
165 60°C. Each sample was run in triplicates. For normalization of gene expression, we used β -actin as a

166 reference gene, and we established a blank control, which was set as 1. Relative gene expression was
167 calculated by using the formula $2^{-\Delta\Delta Ct}$.

168

169 **3. Results**

170 **3.1 Detection of differentially expressed proteins in mice and rats**

171 To find out the effects of *T. gondii* infection in the host brain at the protein level, we infected KM
172 mice and SD rats with *T. gondii* Pru strain. We established an iTRAQ-based strategy to analyze the
173 brains of mice and rats. On the basis of the analysis with ProteinPilot™ 5.0 search engine in the mice
174 and rats respectively, we searched out 173,032 and 166,557 identified spectra, 80,329 and 76,902
175 distinct peptides, 17,081 and 16,974 proteins before grouping, and 5,033 and 4822 proteins with a
176 minimum unused score of > 1.3 (Unused > 1.3), which indicates $> 95\%$ confidence in correct
177 sequence identification. In total, 4,862 and 4,659 proteins were acquired in mice and rats, respectively,
178 with at least two peptides identified (Peptides ≥ 2). About 86.81% and 74.7% of these proteins had a
179 coefficient of variation (CV) of $\leq 50\%$ among replicates in the mice and rats, respectively. All data
180 related to this study has been publicly available on iProX (www.iprox.org) with id IPX0001302000
181 /PXD011192. The following analysis was based on proteins with CV $\leq 50\%$. In total, we determined
182 461 DEPs ($P < 0.05$, FC ≥ 2 , and FC ≤ 0.5) in infected mice, among them 215 were upregulated
183 (46.63%), and 246 downregulated (53.37%). Whereas, in infected rats 292 DEPs were detected ($P <$
184 0.05 , FC ≥ 2 , and FC ≤ 0.5), among them 95 upregulated (32.53%), and 197 downregulated (67.47%)
185 (shown in supplementary information). Considering the names of mice's proteins, which differ from
186 rat's, we used the "BLAST" software to find homogeneous DEPs (HDEPs), which included 381

187 proteins in KM mice and 269 in rats (Figure 1). These results suggested that the DEPs of our focus
188 should be further narrowed so that the cerebral proteomic differences between rats and mice infected
189 with *T. gondii* could be displayed more directly. In addition, further studies should be needed to verify
190 the reliability of the DEPs.

191

192 **3.2 Validation of differentially expressed proteins by quantitative real-time PCR**

193 To determine the reliability of the iTRAQ results in mouse and rat, we selected 5 proteins with
194 different expression level for qRT-PCR analysis. We found total agreement between the results of
195 qRT-PCR and iTRAQ results (Figure 2). Data were statistically analyzed and were presented as a
196 mean \pm standard deviation. The differences in protein expression patterns could be possibly argued
197 by the higher sensitivity of iTRAQ comparing to qRT-PCR suggesting that the iTRAQ results are
198 more reliable.

199

200 **3.3 Complement component 3 upregulation in mice infected with *T. gondii***

201 Because of the massive number of data, we had to reduce the amount of information if we wanted to
202 make a differential analysis. To find the key proteins that differentiate the phenotypes of the two hosts,
203 we firstly, compared the HDEPs from rats and mice (Figure 3a). Sixty-seven HDEPs were detected
204 to be common to both two hosts, while 202 and 314 HDEPs were specific to SD rats and KM mice,
205 respectively. To explore the mechanism of differential susceptibility, we therefore focused on the
206 particular HDEPs. Subsequently, we further investigated biological functions of these HDEPs and
207 mapped them into 71 pathways of rats, 37 pathways of KM mice and 28 homo-pathways using

208 DAVID database. Performing Venn analysis of all these pathways, we further narrowed the range of
209 data to find specific protein pathways in rats and mice (Figure 3b). We focused only on specific
210 pathways of typical HDEPs. We identified 10 mouse-specific pathways and 44 rat-specific pathways,
211 of which the top 10 enriched pathways are shown in Figure 4. The top 10 enriched pathways of rats
212 were Rap1 signaling pathway, Endocytosis, Neurotrophin signaling pathway, Cholinergic synapse,
213 Alcoholism, Ras signaling pathway, Chemokine signaling pathway, GnRH signaling pathway,
214 Melanogenesis, and Alzheimer's disease. Whereas, the top 10 enriched pathways of mice were Protein
215 processing in endoplasmic reticulum, TJ, Complement and coagulation cascades, Parkinson's disease,
216 Platelet activation, Glutathione metabolism, Phosphatidylinositol signaling system, Bacterial
217 invasion of epithelial cells, Amoebiasis, and *Staphylococcus aureus* infection. Upon infection, the
218 parasites persist as intraneuronal cysts in the CNS for the lifetime of the host^[7]. Interestingly, the *T.*
219 *gondii* cysts are more frequently found in the brain of mice than in the brain of rats^[9, 12]. The control
220 of cysts depends on the immune system of hosts, and the ongoing inflammation is required to control
221 *T. gondii* in chronic cerebral infection^[7]. The complement system contributes to the defense of
222 infection, as an important aspect of host immune system^[17]. Additionally, the brain invasion of *T.*
223 *gondii* relates to TJ^[18]. Consequently, we considered that the primary cause of the phenotypic
224 difference between mouse and rat may be associated to the immune system and the brain invasion of
225 *T. gondii*. So we focused on the complement and coagulation cascades pathway and TJ, which had 9
226 and 10 DEPs, respectively (Table 1 and 2). The most significant HDEP among them was C3 therefore,
227 these results suggested that the C3 protein may be a crucial protein that differentiate the phenotype
228 of the two hosts.

229

230 **4. Discussion**

231 In this study, we infected rats and mice with type II *T. gondii* strain (Pru). We then used an iTRAQ-
232 based strategy to identify 381 HDEPs in rats' brain and 269 in KM mice's brains (Figure 1). By using
233 the KEGG pathway analyses, we specifically found the complement-related pathway and TJ pathway
234 in the infected mice's brains, which contained 19 HDEPs. Among them, expression of C3 was
235 increased 11 times as compared with the control group (Table 1 and 2).

236

237 Strain type, host genetic background, and route of infection contribute obviously to the differential
238 susceptibility to *T. gondii* infection^[19]. Because of the differences in the virulence and geographical
239 occurrence, this parasite contains three major types: I, II, and III^[19, 20]. Type II strains are the most
240 prevalent in the United States and Europe^[21]. Mice are good models for *T. gondii* due to their high
241 sensitivity to many different strains^[8]. Type I *T. gondii* strains can lethally infect mice, while type II
242 and III strains cause chronic-progressive or latent infection^[2, 22]. Comparatively, rats are more
243 resistant to toxoplasmosis and mimic *T. gondii* disease in human^[8]. Type I, type II and III strains
244 cause chronic subclinical infection in immunocompetent rats^[9, 10, 23-25], but the pathology and
245 physiology of *T. gondii* infection in rats are still poorly understood^[11]. Taken together, type II strains
246 are appropriate experimental materials to study the different outcome of *T. gondii* infection in mice
247 and rats.

248

249 Scientists attribute the increasing understanding of *T. gondii* protein expression to the advances of

250 proteomic technologies. Using 2-dimensional electrophoresis (2-DE) and matrix-assisted laser-
251 desorption/ionization time of flight mass spectrometry (MALDI- TOF-MS), Cohen *et al.* constructed
252 the first proteome map of *T. gondii* tachyzoite in 2002^[26]. Recently, Zhou *et al.* used the same strategy
253 to observe the proteomic changes in the hippocampus tissue of rat brain with chronic *T. gondii*
254 infection^[27]. Furthermore, Zhou *et al.* explored the proteomic profiles of brain tissues of KM mice at
255 7, 14, 21 d after infection with Pru strain cysts^[28]. Some researchers used two-dimensional difference
256 gel electrophoresis (2D-DIGE) and MALDI-TOF-MS to identify DEPs of 4 different genotypes of *T.*
257 *gondii* tachyzoites^[29]. In recent years, iTRAQ was reported to be the most accurate labeling method
258 for quantification of the relative abundance of proteins with good accuracy and repeatability^[30].
259 Because of its high-throughput, it has been widely used in proteomics to study the relative and
260 absolute quantification of up to 8 samples at the same time^[30]. Sahu *et al.* firstly utilized iTRAQ
261 labeling for a global quantitative proteomic study of the proteome profile of human brain that was
262 co-infected with *T. gondii* and HIV^[31]. Later, the liver proteome of the mouse following acute *T.*
263 *gondii* infection and the proteome of *T. gondii* oocysts during sporulation were reported^[32].
264 Interestingly, Wang *et al.* compared DEPs from different stages of *T. gondii* Pru strain, including
265 tachyzoite, bradyzoites-containing cyst, and sporulated oocyst^[33]. Moreover, we have previously
266 reported the DEPs of *Mongolian gerbil* brains infected with *T. gondii*^[34]. Notably, the new research
267 technology of iTRAQ has provided improvements in three aspects: high throughput, sensitivity and
268 accuracy^[35]. With the advancement of the technology, iTRAQ is still widely used in bio-materials
269 such as microbes, animals, plants and biomedicine^[36]. Most importantly, iTRAQ-based strategy has
270 been used for the identification of biomarkers in a plethora of diseases^[37]. A recent study, validated

271 the role of CD44 in hosts chronically infected with *T. gondii* based on iTRAQ technology, and
272 reported that CD44 mediates the production of IFN- γ and Ca²⁺, and the parasite prefers to invade
273 cells with high levels of CD44^[38]. In brief, this is the first study to establish an iTRAQ-based strategy
274 to compare DEPs from infected rats' and KM mice's brains, which aimed to explore the mechanism
275 of different susceptibility of mice and rats to *T. gondii*.

276

277 *T. gondii* can infect a variety of tissues including the brain, and because of preference for the neurons,
278 it results in *Toxoplasma* encephalitis (TE)^[7]. TE, characterized by both focal and diffuse neurological
279 lesions, concurs with behavior disorders and mental symptoms, such as schizophrenia, Alzheimer's
280 disease (AD) and Parkinson's disease (PD)^[39]. In agreement, *T. gondii*-infected rodents exhibit a
281 number of modifications in their behavior. For example, *T. gondii* causes a shift in the emotional
282 response of rats and increases the timidity in mice^[24, 40]. Most notably, they display an altered
283 response to feline predator odor, from aversion to attraction^[23, 41]. At present, the proposed hypotheses
284 of TE pathogenesis include host dopamine pathways, direct damages to neurons, and parasite-
285 mediated acetylation^[7, 42], but the mechanisms explaining how *T. gondii* exactly affects the CNS are
286 not precisely demonstrated. During *T. gondii* chronic infection, the cysts persist in the CNS for the
287 life time of the host^[43]. The changes observed in the hosts with *T. gondii* on the CNS are related to
288 the tissue cyst tropism, size and number^[44]. Compared to rats, the behavioral disorders of mice are
289 much more conspicuously affected by a *T. gondii*-infection^[14]. Because of the interest in behavioral
290 effects of hosts infected with *T. gondii*, several authors have claimed that the parasite shows a tissue
291 tropism for the amygdalar region in the brains of chronically infected rodents ^[23, 24, 45]. However,

292 amygdala tropism is not clear for tissue cysts in rats^[11]. In addition, some previous studies in mice
293 reported that tissue cysts are distributed unevenly in all regions of the brain with no specific tropism
294 to amygdaloid regions^[13]. But other studies indicated that tissue cyst distribution is not random and
295 tropism could vary with the duration of infection^[44, 46]. Dubey *et al.* (2016) indicated that these
296 differences of tissue cyst tropism are related to techniques, host, parasite strain, route of infection,
297 duration of infection, number of rodents, method of infection and development stage of the parasite^[11].
298 Consequently, in order to avoid tropism differences between mice and rats to influence the proteomic
299 results, we used the same parasite strain (Pru) freshly collected in one mouse, infected animals
300 through the same way (oral), and included the whole brain of each experimental animal after 30 days
301 of infection. Dubey *et al.* (2016) added that the tissue cyst size is dependent on the duration of
302 infection, the type of host cell parasitized, development strain of the parasite and the cytological
303 method used for measurement^[11]. When both hosts are given the same inoculum, tissue cysts in brains
304 of rats are of the same size as in mice^[25]. However, the *T. gondii* cysts are abundantly found in the
305 brain of mice but less frequently found in the brain of rats^[9, 12]. According to a research on reactivation
306 of latent infection, *T. gondii* tachyzoites are present in the brains of chronically infected mice but the
307 frequency of the phenomenon is unknown^[47]. Instead, in experimentally infected rats, tissue cyst
308 rupture was frequent, but there was no evidence for reactivation and the presence of tachyzoites^[11].
309 Moreover, the rats have lower brain infestation and no visible histological damages^[12, 13]. These
310 phenomena of *T. gondii* infection brought us to consider what differences exist between rat and mouse
311 brain.

312

313 The infiltrating peripheral immune cells in the CNS provide a continuous immune response to prevent
314 TE and avoid reactivation of TE^[48]. Since the 1980s, some researchers have shown that the
315 complement pathway is either a critical response factor for an initial immune response to *T. gondii*
316 or a target for parasite evasion^[49]. These observations support that complement pathways are
317 particularly changed in the KM mice brain with *T. gondii* infection, unlike in rats, and it may explain
318 at least partially why mice and rats have different susceptibility to *T. gondii* infection. Previous
319 reports showed that C1q, C3, and C4b are upregulated in some brain disorders associated with TE,
320 including schizophrenia, AD, aging and multiple sclerosis^[34, 50, 51]. In the current study, we identified
321 several pathways, like the AD in the rat and PD in the mice (Figure 4), which is in agreement with
322 the previous studies. Although Xiao *et al.* (2016) have reported alterations in the level of C1q in
323 mice^[52], this is the first study that directly identified C1q, C3, and C4b from the brain of infected KM
324 mice.

325

326 Complement is an innate immune system pathway recognizing and eliminating cellular debris and
327 pathogens. Among them, C1q is a part of the C1-complex and is an immune protein that bridges
328 adaptive and innate immunity. The basic functions of C1q are to clear antigen-antibody immune
329 complexes in systemic circulation^[53]. Furthermore, C1q initiate the proteolytic reactions to generate
330 molecules, which participate in phagocytic responses and inflammation, and induce the activation of
331 the classical complement pathway^[17]. In the classic immune responses, C1q leads to activation of
332 C3 and cleaves C3 into C3a and C3b, which is a central protein in the complement and coagulation
333 cascade^[54]. C3a can promote inflammatory responses and gliosis, which is an anaphylatoxin. C1q

334 and C3b fragments can bind to the surface proteins of microorganisms to promote phagocytosis^[55].
335 Additionally, C1q-C3 can modulate the expression of the interleukin 1 beta (IL1 β) and tumor necrosis
336 factor alpha (TNF α), and the hyperplasia of microglia and astrocytes^[56,57], after SE or in epilepsy^[58].
337 Considering studies on the classical complement pathway in *T. gondii* infection using quantitative
338 PCR, Xiao *et al.* (2016) firstly claimed that C1q activation is a part of the host immune response to
339 *T. gondii* chronic infection, and primarily recognizes degenerate cysts as targets for the parasite
340 elimination^[52]. In our study, we used iTRAQ strategy to confirm the variation of C1q in the KM mice
341 with *T. gondii* infection. As a factor for SE or epilepsy, the *T. gondii* increases C1q and C3 in the host
342 brain, which may remarkably contribute to the neurogenic inflammation.

343

344 For non-inflammatory mechanisms, on the one hand, microglia express complement receptors, and
345 C1q, while C3 locate synapses, which collectively mediate phagocytic microglia to prune synapses
346 in developing brains^[59]. However, this process is significantly down-regulated in the mature brain^[59].
347 C4 also is a crucial part of the complement cascade, which is expressed by neurons and is secreted
348 by dendrites, axons and synapses^[51]. During postnatal development, C4 promotes synapse
349 elimination in mice^[59]. Accordingly, C4 activity in the event of schizophrenia will reduce the number
350 of synapses^[51, 60]. Emerging research implicates activation of the synaptic pruning pathway in
351 synapses loss in the AD brain^[61]. Accordingly, we hypothesized that by increasing C1q, C4b, and C3
352 expression, chronic *T. gondii* infection mediates damage of nerve cells, such as neurodegeneration,
353 possible synapse loss, and neuronal death. On the other hand, C1q and iC3b proteins can mediate
354 phagocytic responses of microglia, which consequently, means that C1q and iC3b attract microglia

355 to the orchestrate elimination of foreign bodies, called as “eat-me” signals ^[17, 62]. To illustrate, C1q
356 binds to cellular debris or apoptotic cells to promote microglial clearance and prevent further
357 inflammation^[56, 63]. Therefore, some researchers reported that the activation of complement protects
358 nerve cells in epilepsy and SE^[64]. For *T. gondii* infection, this mechanism may protect the nerve cells
359 as well. In conclusion, the complement is a two-edged weapon, which can be beneficial and
360 detrimental for the host when *T. gondii* infects the brain.

361

362 The basal lamina, pericytes, endothelial cells and astrocytic end-feet comprise the BBB, which is a
363 selective barrier. The tight junctions in the BBB are adhesive structures that seal the gap between
364 endothelial cells to selectively prevent the entry into the brain of pathogenic microbes and antigens
365 from the blood^[65]. Pathogens must cross the BBB to enter the CNS, which is a challenge^[66]. A
366 plausible explanation for the development of TE is that some *T. gondii* tachyzoites enter the CNS and
367 form into cysts to avoid the host immune responses and anti-toxoplasma drugs. Nevertheless, how
368 does *T. gondii* cross TJs to enter the brain? Two mechanisms have been proposed. The first one is the
369 transcellular crossing mechanism, in which tachyzoites from the bloodstream can adhere to, invade,
370 replicate and pass from the endothelial cells of CNS to the CNS parenchyma. This mechanism was
371 discovered by utilizing multiphoton *in vivo* imaging and transgenic reporter systems (Figure 5B) ^[6].
372 Although the parasite infection of the CNS precedes immune cells infiltration^[67], some studies
373 reported that mouse brain is more quickly infected by dendritic cells and macrophages previously
374 infected with *T. gondii* tachyzoites than by *T. gondii* tachyzoites only^[68]. This findings are in
375 agreement with a second mechanism called the Trojan-horse like mechanism, which implicates

376 infected immune cells as a carriers of the intracellular parasites through the BBB (Figure 5A)^[5, 68]. In
377 addition, we thought of a third mechanism in which *T. gondii* tachyzoites may directly cross the BBB
378 through the brain TJ (Figure 5C). Previous studies have described that the *T. gondii* tachyzoites can
379 show “gliding motility”, which can help the parasites to go across the epithelium of the small
380 intestine^[69]. Inspiringly, under shear force conditions tachyzoites can adhere to the human vascular
381 endothelium to increase the invasive percentage^[70]. These lines of evidence prompted us to wonder
382 if *T. gondii* crosses the BBB via the intercellular space. Some scholars named it as ‘paracellular entry’
383 ^[71], but until now, no study presented direct evidence to support it.

384

385 We hypothesized that *T. gondii* disrupts the TJ of BBB and allows *T. gondii* to pass into the brain by
386 paracellular entry, in which C3 plays a crucial role. Previous studies reported that C3 disrupts the
387 renal tubules barrier to develop proteinuria ^[72, 73]. In brains, blood-cerebrospinal fluid (CSF) barrier
388 is as vital as the BBB, where the choroid plexus epithelial (CPEpi) cells represent an essential
389 component of this barrier. Additionally, the CPEpi cells express the C3a receptor (C3aR) of C3,
390 which is a G protein-coupled receptor^[74]. Moreover, myosin light-chain kinase (MLCK) is a key
391 regulator of TJ permeability, and by the addition of C3a, it transiently increases its phosphorylation
392 ^[75]. C3a was proved by immunofluorescence to be able to disorganize the TJ of mouse CPE. This
393 effect of C3a was also found in the renal and pulmonary epithelia^[73, 76]. It represents one line of
394 evidence for our hypothesis of the involvement of TJ pathway in KM mouse brain during *T. gondii*
395 infection. Transmembrane proteins compose TJs, including occludins, claudins, and intracellular
396 proteins, which maintain the integrity of the BBB. These intracellular proteins contain ZO-1, ZO-2

397 and ZO-3^{[77][78]}. Moreover, Protein kinase C (PKC) is essential for the normal assembly of TJs. PKC
398 affects the opening of TJs and plays a role in decreasing and increasing the permeability of TJ^[79].
399 Phorbol 12-myristate 13-acetate as an agonist of PKC can lead to the TJs disintegration^[80]. Persistent
400 activation of PKC α decreases the expression of TJ proteins and increases the BBB permeability,
401 which means that the barrier function is lost^[81]. In this study, the TJ pathway, and majority of HDEPs
402 were down-regulated such as the PKC, however a few HDEPs were up-regulated; TJ protein zonula
403 occludens-2 (ZO-2) was one of them. This up-regulation may be a compensatory effect of the TJ
404 damage caused by *T. gondii* infection, which induces the PKC down-regulation to stimulate the
405 secretion of TJ protein, in order to restore the TJ functionality.

406

407 In other contexts, the pharmacologic interventions of complement cascade especially in C3 has been
408 explored such as autoimmune arthritis^[82] and reactive airway disease^[83]. Our findings elicit lots of
409 significant questions for further studies. Complement C3 manipulation of the BBB integrity might be
410 employed to allow for increased access of *T. gondii* into the CNS. Further preclinical studies could
411 make this hypothesis possible.

412

413 **Conflict of interest**

414 The authors declare that they have no competing interests.

415

416 **Acknowledgements**

417 This work was supported, in part, by grants from the national key research and development program

418 of China (2017YFD0501305), Major scientific research projects (characteristic innovation) of
419 Guangdong Province (2017KTSCX018), the Guangzhou Zoo Project (h2016141), the Natural
420 Science Foundation of Guangdong Province (2016A030313396), and Huizhou science and
421 technology projects (2015B040009001). The authors acknowledge the efforts of Prof. Virginia
422 Aragon [IRTA, Centre de Recerca en Sanitat Animal (CRESA-IRTA), Barcelona, Spain] for her
423 contribution in proofreading of this work.

424

425 **References**

- 426 [1] D. E. Hill, S. Chirukandoth, J. P. Dubey, *Animal health research reviews* 2005, 6, 41.
- 427 [2] J. C. Boothroyd, M. E. Grigg, *Current opinion in microbiology* 2002, 5, 438.
- 428 [3] J. G. Montoya, O. Liesenfeld, *Lancet* (London, England) 2004, 363, 1965.
- 429 [4] B. J. Luft, J. S. Remington, *Clinical infectious diseases : an official publication of the Infectious Diseases Society*
430 *of America* 1992, 15, 211.
- 431 [5] N. Courret, S. Darche, P. Sonigo, G. Milon, D. Buzoni-Gatel, I. Tardieux, *Blood* 2006, 107, 309.
- 432 [6] C. Konradt, N. Ueno, D. A. Christian, J. H. DeLong, G. H. Pritchard, J. Herz, D. J. Bzik, A. A. Koshy, D. B. McGavern,
433 M. B. Lodoen, C. A. Hunter, *Nature microbiology* 2016, 1, 16001.
- 434 [7] N. Blanchard, I. R. Dunay, D. Schluter, *Parasite immunology* 2015, 37, 150.
- 435 [8] E. A. Innes, *Comparative immunology, microbiology and infectious diseases* 1997, 20, 131.
- 436 [9] J. P. Dubey, J. K. Frenkel, *Veterinary parasitology* 1998, 77, 1.
- 437 [10] J. P. Dubey, S. K. Shen, O. C. Kwok, J. K. Frenkel, *The Journal of parasitology* 1999, 85, 657.
- 438 [11] J. P. Dubey, L. R. Ferreira, M. Alsaad, S. K. Verma, D. A. Alves, G. N. Holland, G. A. McConkey, *PloS one* 2016,
439 11, e0156255.
- 440 [12] J. Babaie, M. Sayyah, S. Choopani, T. Asgari, M. Golkar, K. Gharagozli, *Epilepsy research* 2017, 135, 137.
- 441 [13] M. Berenreiterova, J. Flegr, A. A. Kubena, P. Nemeč, *PloS one* 2011, 6, e28925.
- 442 [14] P. A. Witting, *Zeitschrift für Parasitenkunde* (Berlin, Germany) 1979, 61, 29.
- 443 [15] P. K. Smith, R. I. Krohn, G. T. Hermanson, A. K. Mallia, F. H. Gartner, M. D. Provenzano, E. K. Fujimoto, N. M.
444 Goeke, B. J. Olson, D. C. Klenk, *Analytical biochemistry* 1985, 150, 76.
- 445 [16] J. R. Wisniewski, A. Zougman, N. Nagaraj, M. Mann, *Nature methods* 2009, 6, 359.

- 446 [17] S. R. Barnum, *Pharmacology & therapeutics* 2017, 172, 63.
- 447 [18] E. A. Wohlfert, I. J. Blader, E. H. Wilson, *Trends in parasitology* 2017, 33, 519.
- 448 [19] J. P. Saeij, J. P. Boyle, J. C. Boothroyd, *Trends in parasitology* 2005, 21, 476.
- 449 [20] T. Lehmann, P. L. Marcet, D. H. Graham, E. R. Dahl, J. P. Dubey, *Proceedings of the National Academy of Sciences*
450 *of the United States of America* 2006, 103, 11423.
- 451 [21] C. Su, A. Khan, P. Zhou, D. Majumdar, D. Ajzenberg, M. L. Darde, X. Q. Zhu, J. W. Ajioka, B. M. Rosenthal, J. P.
452 Dubey, L. D. Sibley, *Proceedings of the National Academy of Sciences of the United States of America* 2012, 109, 5844;
453 E. K. Shwab, X. Q. Zhu, D. Majumdar, H. F. Pena, S. M. Gennari, J. P. Dubey, C. Su, *Parasitology* 2014, 141, 453.
- 454 [22] D. K. Howe, L. D. Sibley, *The Journal of infectious diseases* 1995, 172, 1561.
- 455 [23] A. Vyas, S. K. Kim, N. Giacomini, J. C. Boothroyd, R. M. Sapolsky, *Proceedings of the National Academy of*
456 *Sciences of the United States of America* 2007, 104, 6442.
- 457 [24] L. E. Gonzalez, B. Rojnik, F. Urrea, H. Urdaneta, P. Petrosino, C. Colasante, S. Pino, L. Hernandez, *Behavioural*
458 *brain research* 2007, 177, 70.
- 459 [25] J. P. Dubey, *The Journal of parasitology* 1996, 82, 951.
- 460 [26] A. M. Cohen, K. Rumpel, G. H. Coombs, J. M. Wastling, *International journal for parasitology* 2002, 32, 39.
- 461 [27] Y. H. Zhou, H. J. Fan, Y. Zhang, Y. Z. Huang, Y. L. Xu, Y. H. Tao, Q. Gao, *Zhongguo ji sheng chong xue yu ji sheng*
462 *chong bing za zhi = Chinese journal of parasitology & parasitic diseases* 2013, 31, 454.
- 463 [28] D. H. Zhou, F. R. Zhao, S. Y. Huang, M. J. Xu, H. Q. Song, C. Su, X. Q. Zhu, *Parasites & vectors* 2013, 6, 96.
- 464 [29] D. H. Zhou, F. R. Zhao, A. J. Nisbet, M. J. Xu, H. Q. Song, R. Q. Lin, S. Y. Huang, X. Q. Zhu, *Electrophoresis* 2014,
465 35, 533.
- 466 [30] W. W. Wu, G. Wang, S. J. Baek, R. F. Shen, *Journal of proteome research* 2006, 5, 651.
- 467 [31] A. Sahu, S. Kumar, S. K. Sreenivasamurthy, L. D. Selvan, A. K. Madugundu, S. D. Yelamanchi, V. N. Puttamallesh,
468 G. Dey, A. K. Anil, A. Srinivasan, K. K. Mukherjee, H. Gowda, P. Satishchandra, A. Mahadevan, A. Pandey, T. S. Prasad,
469 S. K. Shankar, *Clinical proteomics* 2014, 11, 39.
- 470 [32] C. X. Zhou, X. Q. Zhu, H. M. Elsheikha, S. He, Q. Li, D. H. Zhou, X. Suo, *Journal of proteomics* 2016, 148, 12; J.
471 J. He, J. Ma, H. M. Elsheikha, H. Q. Song, D. H. Zhou, X. Q. Zhu, *PloS one* 2016, 11, e0152022.
- 472 [33] Z. X. Wang, C. X. Zhou, H. M. Elsheikha, S. He, D. H. Zhou, X. Q. Zhu, *Frontiers in microbiology* 2017, 8, 985.
- 473 [34] L. Lv, Y. Wang, W. Feng, J. A. Hernandez, W. Huang, Y. Zheng, X. Zhou, S. Lv, Y. Chen, Z. G. Yuan, *Journal of*
474 *proteomics* 2017, 160, 74.
- 475 [35] S. Ma, Y. Sun, X. Zhao, P. Xu, *Sheng wu gong cheng xue bao = Chinese journal of biotechnology* 2014, 30, 1073.
- 476 [36] L. Zhang, P. Qiang, J. Yu, Y. Miao, Z. Chen, J. Qu, Q. Zhao, Z. Chen, Y. Liu, X. Yao, B. Liu, L. Cui, H. Jing, G. Sun,

477 Autophagy 2018; L. Song, Y. Gao, J. Li, L. Ban, *Frontiers in physiology* 2018, 9, 1016; D. Tian, L. Yang, Z. Chen, Z.
478 Chen, F. Wang, Y. Zhou, Y. Luo, L. Yang, S. Chen, *Rice (New York, N.Y.)* 2018, 11, 47; X. Lin, T. Liu, P. Li, Z. He, Y.
479 Zhong, H. Cui, J. Luo, Y. Wang, T. Tang, *BioMed research international* 2018, 2018, 6920213; R. Sun, G. Cui, Y. Chen,
480 B. Shu, G. Zhong, X. Yi, *Proteomics* 2018, e1800192; M. Li, X. Wu, X. Guo, P. Bao, X. Ding, M. Chu, C. Liang, P. Yan,
481 *Proteome science* 2018, 16, 14; H. Wang, H. Wei, L. Tang, J. Lu, C. Mu, C. Wang, *Gene* 2018; H. Zhou, Y. Kang, Z. Shi,
482 L. Lu, X. Li, T. Chu, J. Liu, L. Liu, Y. Lou, C. Zhang, G. Ning, S. Feng, X. Kong, *Gene* 2018; W. Ye, W. Zhang, T. Liu,
483 M. Zhu, S. Li, H. Li, Z. Huang, X. Gao, *Proteomics* 2018, e1800023.

484 [37] J. Shan, Z. Sun, J. Yang, J. Xu, W. Shi, Y. Wu, Y. Fan, H. Li, *Oral diseases* 2018; A. Swiatly, A. Horala, J. Matysiak,
485 J. Hajduk, E. Nowak-Markwitz, Z. J. Kokot, *International journal of molecular sciences* 2018, 19; D. L. Fernandez-Coto,
486 J. Gil, A. Hernandez, R. Herrera-Goepfert, I. Castro-Romero, E. Hernandez-Marquez, A. S. Arenas-Linares, V. T.
487 Calderon-Sosa, M. A. Sanchez-Aleman, A. Mendez-Tenorio, S. Encarnacion-Guevara, G. Ayala, *Journal of proteomics*
488 2018, 186, 15.

489 [38] J. Yang, F. Du, X. Zhou, L. Wang, S. Li, R. Fang, J. Zhao, *Parasitology research* 2018, 117, 2623.

490 [39] S. Fabiani, B. Pinto, U. Bonuccelli, F. Bruschi, *Journal of the neurological sciences* 2015, 351, 3.

491 [40] J. Hay, W. M. Hutchison, P. P. Aitken, D. I. Graham, *Annals of tropical medicine and parasitology* 1983, 77, 483; W.
492 M. Hutchinson, M. Bradley, W. M. Cheyne, B. W. Wells, J. Hay, *Annals of tropical medicine and parasitology* 1980, 74,
493 337.

494 [41] M. Berdoy, J. P. Webster, D. W. Macdonald, *Proceedings. Biological sciences* 2000, 267, 1591; J. P. Webster,
495 *Schizophrenia bulletin* 2007, 33, 752.

496 [42] F. Haroon, U. Handel, F. Angenstein, J. Goldschmidt, P. Kreutzmann, H. Lison, K. D. Fischer, H. Scheich, W. Wetzel,
497 D. Schluter, E. Budinger, *PloS one* 2012, 7, e35516; E. Prandovszky, E. Gaskell, H. Martin, J. P. Dubey, J. P. Webster, G.
498 A. McConkey, *PloS one* 2011, 6, e23866.

499 [43] J. P. Dubey, J. K. Frenkel, *The Journal of protozoology* 1976, 23, 537.

500 [44] C. Afonso, V. B. Paixao, R. M. Costa, *PloS one* 2012, 7, e32489.

501 [45] G. A. McConkey, H. L. Martin, G. C. Bristow, J. P. Webster, *The Journal of experimental biology* 2013, 216, 113.

502 [46] J. Gatkowska, M. Wiczorek, B. Dziadek, K. Dzitko, H. Dlugonska, *Parasitology research* 2012, 111, 53; T. C.
503 Melzer, H. J. Cranston, L. M. Weiss, S. K. Halonen, *Journal of neuroparasitology* 2010, 1.

504 [47] J. P. Dubey, C. A. Speer, S. K. Shen, O. C. Kwok, J. A. Blixt, *The Journal of parasitology* 1997, 83, 870.

505 [48] J. P. Nance, K. M. Vannella, D. Worth, C. David, D. Carter, S. Noor, C. Hubeau, L. Fitz, T. E. Lane, T. A. Wynn, E.
506 H. Wilson, *PLoS pathogens* 2012, 8, e1002990.

507 [49] R. D. Schreiber, H. A. Feldman, *The Journal of infectious diseases* 1980, 141, 366; S. A. Fuhrman, K. A. Joiner,

508 Journal of immunology (Baltimore, Md. : 1950) 1989, 142, 940; D. Sacks, A. Sher, Nature immunology 2002, 3, 1041.

509 [50] I. Michailidou, J. G. Willems, E. J. Kooi, C. van Eden, S. M. Gold, J. J. Geurts, F. Baas, I. Huitinga, V. Ramaglia,

510 Annals of neurology 2015, 77, 1007; E. G. Severance, K. L. Gressitt, S. L. Buka, T. D. Cannon, R. H. Yolken,

511 Schizophrenia research 2014, 159, 14; A. H. Stephan, D. V. Madison, J. M. Mateos, D. A. Fraser, E. A. Lovelett, L.

512 Coutellier, L. Kim, H. H. Tsai, E. J. Huang, D. H. Rowitch, D. S. Berns, A. J. Tenner, M. Shamloo, B. A. Barres, The

513 Journal of neuroscience : the official journal of the Society for Neuroscience 2013, 33, 13460.

514 [51] A. Sekar, A. R. Bialas, H. de Rivera, A. Davis, T. R. Hammond, N. Kamitaki, K. Tooley, J. Presumey, M. Baum, V.

515 Van Doren, G. Genovese, S. A. Rose, R. E. Handsaker, M. J. Daly, M. C. Carroll, B. Stevens, S. A. McCarroll, Nature

516 2016, 530, 177.

517 [52] J. Xiao, Y. Li, K. L. Gressitt, H. He, G. Kannan, T. L. Schultz, N. Svezhova, V. B. Carruthers, M. V. Pletnikov, R. H.

518 Yolken, E. G. Severance, Brain, behavior, and immunity 2016, 58, 52.

519 [53] M. J. Walport, The New England journal of medicine 2001, 344, 1058.

520 [54] G. Bajic, S. E. Degn, S. Thiel, G. R. Andersen, The EMBO journal 2015, 34, 2735.

521 [55] N. M. Thielens, F. Tedesco, S. S. Bohlson, C. Gaboriaud, A. J. Tenner, Molecular immunology 2017, 89, 73.

522 [56] D. A. Fraser, K. Pisalyaput, A. J. Tenner, Journal of neurochemistry 2010, 112, 733.

523 [57] E. Hernandez-Encinas, D. Aguilar-Morante, J. A. Morales-Garcia, E. Gine, M. Sanz-SanCristobal, A. Santos, A.

524 Perez-Castillo, Journal of neuroinflammation 2016, 13, 276.

525 [58] M. J. Benson, N. K. Thomas, S. Talwar, M. P. Hodson, J. W. Lynch, T. M. Woodruff, K. Borges, Neurobiology of

526 disease 2015, 76, 87; J. Choi, S. Koh, Yonsei medical journal 2008, 49, 1; L. A. Shapiro, L. Wang, C. E. Ribak, Epilepsia

527 2008, 49 Suppl 2, 33.

528 [59] B. Stevens, N. J. Allen, L. E. Vazquez, G. R. Howell, K. S. Christopherson, N. Nouri, K. D. Micheva, A. K. Mehalow,

529 A. D. Huberman, B. Stafford, A. Sher, A. M. Litke, J. D. Lambris, S. J. Smith, S. W. John, B. A. Barres, Cell 2007, 131,

530 1164; D. P. Schafer, E. K. Lehrman, A. G. Kautzman, R. Koyama, A. R. Mardinly, R. Yamasaki, R. M. Ransohoff, M. E.

531 Greenberg, B. A. Barres, B. Stevens, Neuron 2012, 74, 691.

532 [60] L. J. Garey, W. Y. Ong, T. S. Patel, M. Kanani, A. Davis, A. M. Mortimer, T. R. Barnes, S. R. Hirsch, Journal of

533 neurology, neurosurgery, and psychiatry 1998, 65, 446; J. R. Glausier, D. A. Lewis, Neuroscience 2013, 251, 90.

534 [61] S. Hong, V. F. Beja-Glasser, B. M. Nfonoyim, A. Frouin, S. Li, S. Ramakrishnan, K. M. Merry, Q. Shi, A. Rosenthal,

535 B. A. Barres, C. A. Lemere, D. J. Selkoe, B. Stevens, Science (New York, N.Y.) 2016, 352, 712.

536 [62] D. P. Schafer, E. K. Lehrman, B. Stevens, Glia 2013, 61, 24.

537 [63] K. S. Ravichandran, The Journal of experimental medicine 2010, 207, 1807.

538 [64] R. Dingledine, N. H. Varvel, F. E. Dudek, Advances in experimental medicine and biology 2014, 813, 109; A. L. do

539 Nascimento, N. F. Dos Santos, F. Campos Pelagio, S. Aparecida Teixeira, E. A. de Moraes Ferrari, F. Langone, *Brain*
540 *research* 2012, 1470, 98.

541 [65] K. Shigetomi, J. Ikenouchi, *Journal of biochemistry* 2017.

542 [66] N. J. Abbott, L. Ronnback, E. Hansson, *Nature reviews. Neuroscience* 2006, 7, 41.

543 [67] F. K. Conley, K. A. Jenkins, *Infection and immunity* 1981, 31, 1184.

544 [68] H. Lambert, N. Hitziger, I. Dellacasa, M. Svensson, A. Barragan, *Cellular microbiology* 2006, 8, 1611.

545 [69] J. M. Dobrowolski, L. D. Sibley, *Cell* 1996, 84, 933; I. Tardieux, R. Menard, *Traffic (Copenhagen, Denmark)* 2008,
546 9, 627.

547 [70] K. S. Harker, E. Jivan, F. Y. McWhorter, W. F. Liu, M. B. Lodoen, *mBio* 2014, 5, e01111.

548 [71] O. A. Mendez, A. A. Koshy, *PLoS pathogens* 2017, 13, e1006351.

549 [72] J. Floege, K. Amann, *Lancet (London, England)* 2016, 387, 2036.

550 [73] L. Bao, Y. Wang, M. Haas, R. J. Quigg, *Kidney international* 2011, 80, 524.

551 [74] R. S. Ames, Y. Li, H. M. Sarau, P. Nuthulaganti, J. J. Foley, C. Ellis, Z. Zeng, K. Su, A. J. Jurewicz, R. P. Hertzberg,
552 D. J. Bergsma, C. Kumar, *The Journal of biological chemistry* 1996, 271, 20231.

553 [75] K. E. Cunningham, J. R. Turner, *Annals of the New York Academy of Sciences* 2012, 1258, 34.

554 [76] S. M. Drouin, J. Kildsgaard, J. Haviland, J. Zabner, H. P. Jia, P. B. McCray, Jr., B. F. Tack, R. A. Wetsel, *Journal of*
555 *immunology (Baltimore, Md. : 1950)* 2001, 166, 2025; A. Boire, Y. Zou, J. Shieh, D. G. Macalinao, E. Pentsova, J.
556 Massague, *Cell* 2017, 168, 1101; G. Conyers, L. Milks, M. Conklyn, H. Showell, E. Cramer, *The American journal of*
557 *physiology* 1990, 259, C577; D. Ricklin, E. S. Reis, J. D. Lambris, *Nature reviews. Nephrology* 2016, 12, 383.

558 [77] S. Citi, M. Cordenosi, *Biochimica et biophysica acta* 1998, 1448, 1.

559 [78] J. D. Huber, R. D. Egleton, T. P. Davis, *Trends in neurosciences* 2001, 24, 719.

560 [79] M. L. Chen, C. Pothoulakis, J. T. LaMont, *The Journal of biological chemistry* 2002, 277, 4247; V. Nunbhakdi-Craig,
561 T. Machleidt, E. Ogris, D. Bellotto, C. L. White, 3rd, E. Sontag, *The Journal of cell biology* 2002, 158, 967.

562 [80] S. Citi, N. Denisenko, *Journal of cell science* 1995, 108 (Pt 8), 2917.

563 [81] C. L. Willis, D. S. Meske, T. P. Davis, *Journal of cerebral blood flow and metabolism : official journal of the*
564 *International Society of Cerebral Blood Flow and Metabolism* 2010, 30, 1847.

565 [82] P. Hutamekalin, K. Takeda, M. Tani, Y. Tsuga, N. Ogawa, N. Mizutani, S. Yoshino, *Journal of pharmacological*
566 *sciences* 2010, 112, 56.

567 [83] M. A. Khan, M. R. Nicolls, B. Surguladze, I. Saadoun, *Respiratory medicine* 2014, 108, 543.

568

Table 1: HDEPs of the complement and coagulation cascades pathway in the infected mice's brain.

Protein	Gene symbol	Description	Toxoplasma encephalitis/Control (Fold change)
Plasminogen	Plg	Plasmin is an important enzyme present in blood that degrades many blood plasma proteins, including fibrin clots. The degradation of fibrin is termed fibrinolysis.	5.032887165
Antithrombin-III	Serpinc1	AT III is generally referred to solely as "Antithrombin", which is a small protein molecule that inactivates several enzymes of the coagulation system.	3.018619571
Fibrinogen beta chain	Fgb	Fibrinogen beta chain, also known as FGB, is a gene found in humans and most other vertebrates with a similar system of blood coagulation. The protein encoded by this gene is the beta component of fibrinogen, a blood-borne glycoprotein composed of three pairs of nonidentical polypeptide chains. Following vascular injury, fibrinogen is cleaved by thrombin to form fibrin which is the most abundant component of blood clots.	6.43841143
Fibrinogen alpha chain	Fga	The protein encoded by this gene is the alpha component of fibrinogen.	3.565736133
Coagulation factor XIII A chain	F13a1	Coagulation factor XIII is the last zymogen to become activated in the blood coagulation cascade. Plasma factor XIII is a heterotetramer composed of 2 A subunits and 2 B subunits. The A subunits have catalytic function, and the B subunits do not have enzymatic activity and may serve as plasma carrier molecules.	4.641328363
Alpha-2-macroglobulin-P	A2m	Alpha 2 macroglobulin acts as an antiprotease and is able to inactivate an enormous variety of proteinases. It functions as an inhibitor of fibrinolysis by inhibiting plasmin and kallikrein. It functions as an inhibitor of coagulation by inhibiting thrombin.	10.46278151

Complement C3	C3	Complement component 3, often simply called C3, is a protein of the immune system. It plays a central role in the complement system and contributes to innate immunity.	11.06623745
Complement C4-B	C4b	Complement component 4, in humans, is a protein involved in the intricate complement system, originating from the human leukocyte antigen (HLA) system. It serves a number of critical functions in immunity, tolerance, and autoimmunity with the other numerous components.	9.375619888
Complement C1q subcomponent subunit A	C1qa	The C1q complex is a protein complex involved in the complement system, which is part of the innate immune system. C1q is part of the C1-complex.	5.649369717

Table 2: HDEPs of the Tight junction pathway in the infected mice's brain.

Protein	Gene symbol	Toxoplasma encephalitis/Control (Fold change)	Description
Tight junction protein ZO-2	Tjp2	4.23769481	Tight junction protein ZO-2 plays a role in tight junctions and adherens junctions. It has a role as a scaffold protein which cross-links and anchors Tight Junction (TJ) strand proteins, which are fibril-like structures within the lipid bilayer, to the actin cytoskeleton.
Protein kinase C	Prkca	0.403918909	Protein kinase C modulates membrane structure events.
Protein kinase C gamma type	Prkcg	0.314442886	
Ras-related protein Rab-3B	Rab3b	0.408556377	Ras-related protein Rab-3B plays a role in protein transport.
Alpha-actinin-2	Actn2	0.44870987	As a bundling protein, it is thought to anchor actin to a variety of intracellular structures.
Myosin-9	Myh9	7.139545535	Myosins comprise a superfamily of ATP-dependent motor proteins and are best known for their role in muscle contraction and their involvement in a wide range of other motility processes in eukaryotes. Virtually all eukaryotic cells contain myosin isoforms. During cell spreading, myosin-9 plays an important role in cytoskeleton reorganization, focal contacts formation.
Myosin-10	Myh10	0.355443681	
Myosin-11	Myh11	0.228766571	
Protein Shroom2	Shroom2	0.389755496	Shroom2 is both necessary and sufficient to govern the localization of pigment granules at the apical surface of epithelial cells. It is possible that SHROOM2 mutations may contribute to human visual system disorders.
Catenin alpha-1	Ctnna1	2.592327188	Catenin alpha-1 associates with the cytoplasmic domain of a variety of cadherins. The association of catenins to cadherins produces a complex which is linked to the actin filament network, and which seems to be of primary importance for cadherins cell-adhesion properties.

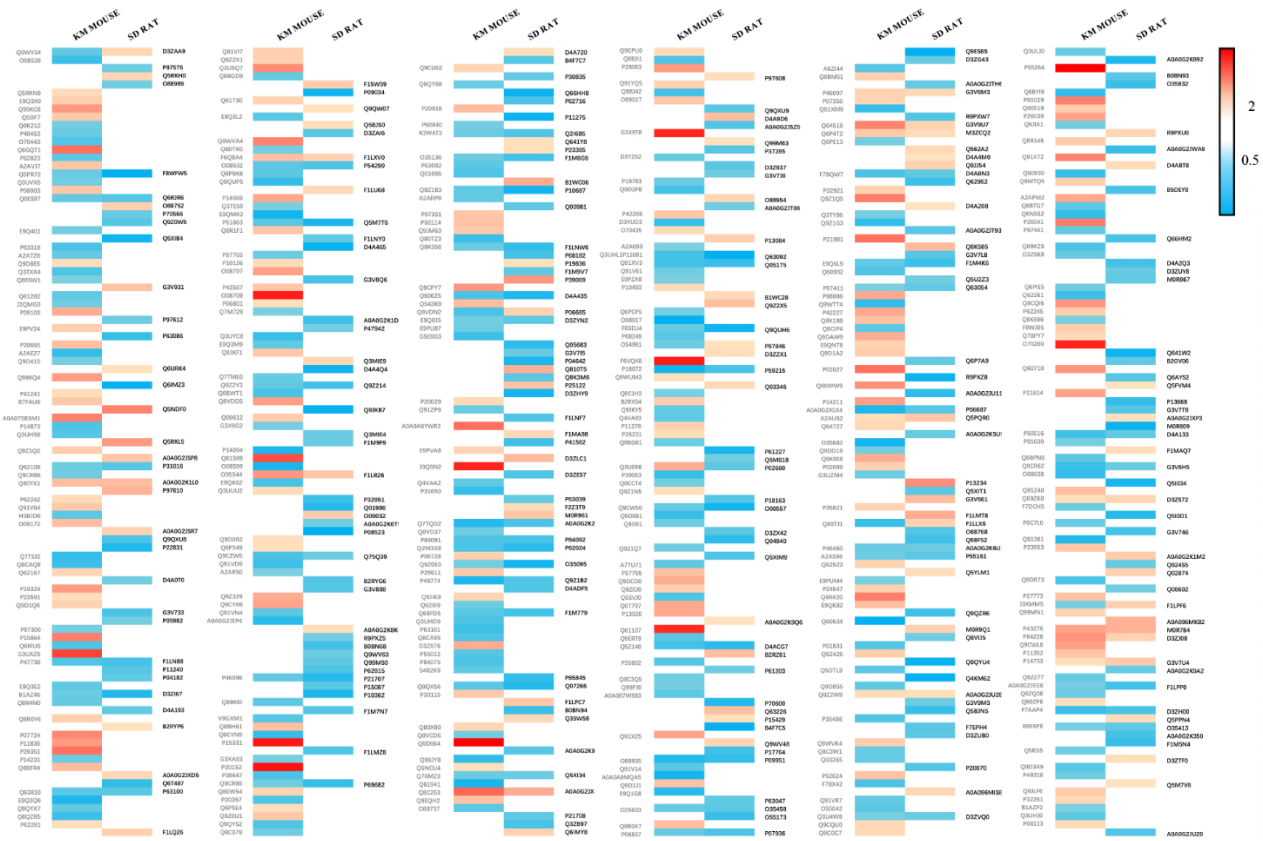


Fig. 1. Heat map of HDEPs. The HDEPs with a fold change of ≥ 2 -fold or ≤ 2 -fold and $p \leq 0.05$ are shown in the heat map, which include 381 proteins in rats and 269 in KM mice.

Upregulation is displayed by orange color and downregulation is displayed by blue color.

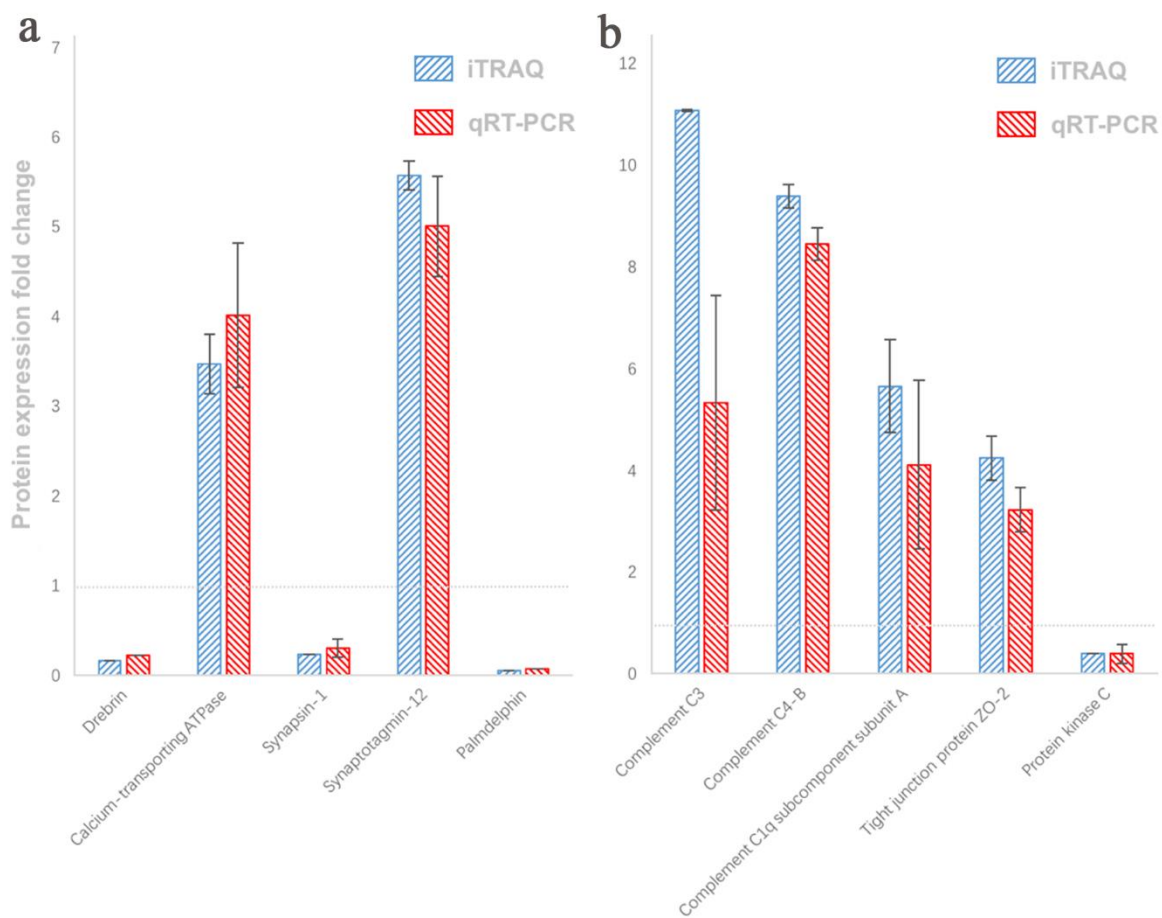


Fig. 2. The fold change in mRNA expression, detected by qRT-PCR. The clustered columns show that the expression patterns of 10 selected proteins detected by qRT-PCR were consistent with those obtained by iTRAQ. (a) The clustered column shows the expression patterns of the SD rats' selected proteins. (b) The clustered column shows the expression patterns of the KM mice's selected proteins. Error bars represent SEM.

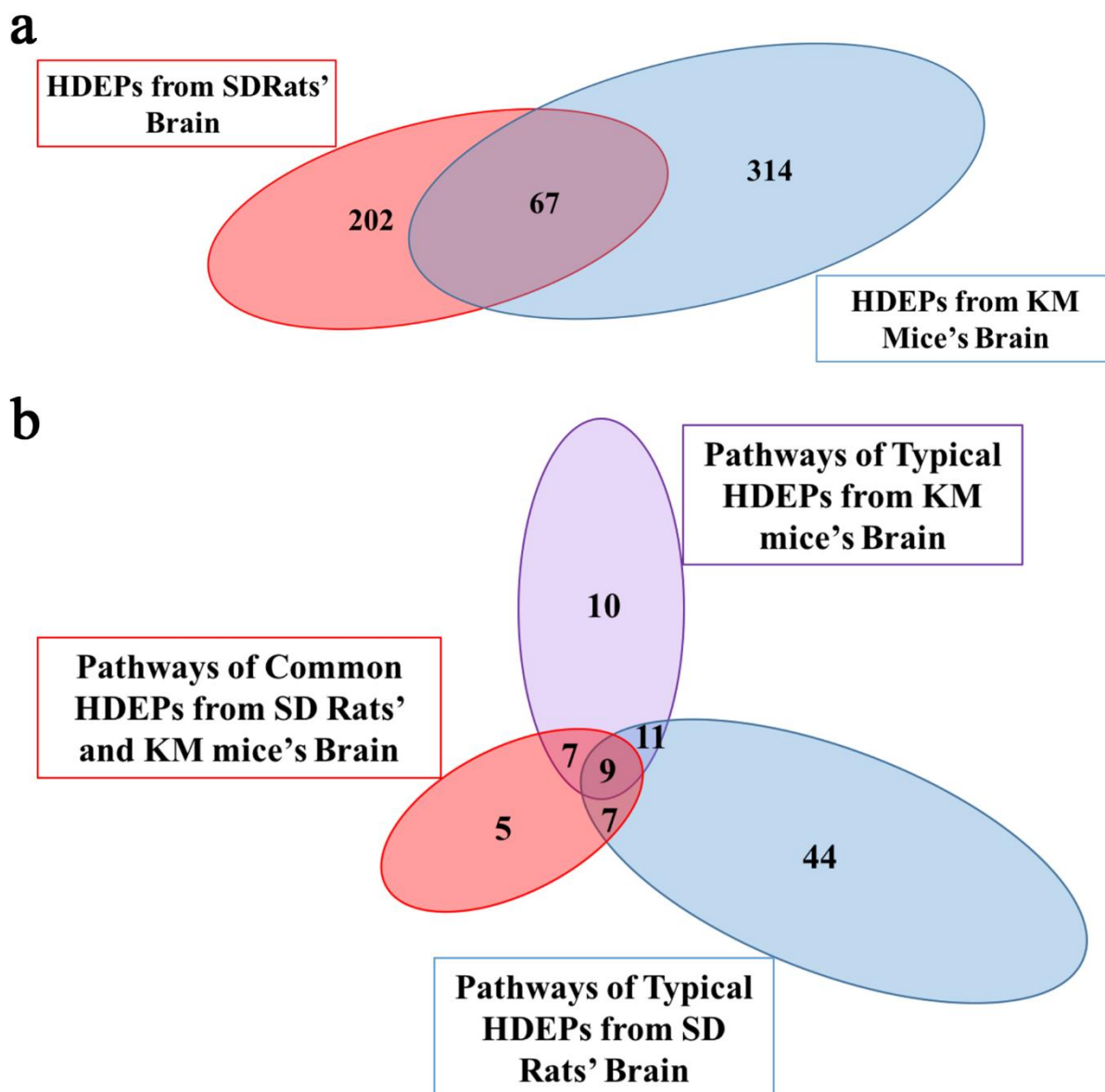


Fig. 3. Comparison of the HDEPs. (a) Venn diagrams of HDEPs between SD rats' and KM mice' brain. Proteins with base mean fold change ≥ 2 or ≤ 2 , and $p < 0.05$ were collected for analysis.

(b) By using the KEGG database, we investigated biological functions of these HDEPs and mapped them to 93 pathways in total. Venn diagrams of pathways of HDEPs between SD rats' and KM mice' brain; $p < 0.01$ were collected for each pathway.

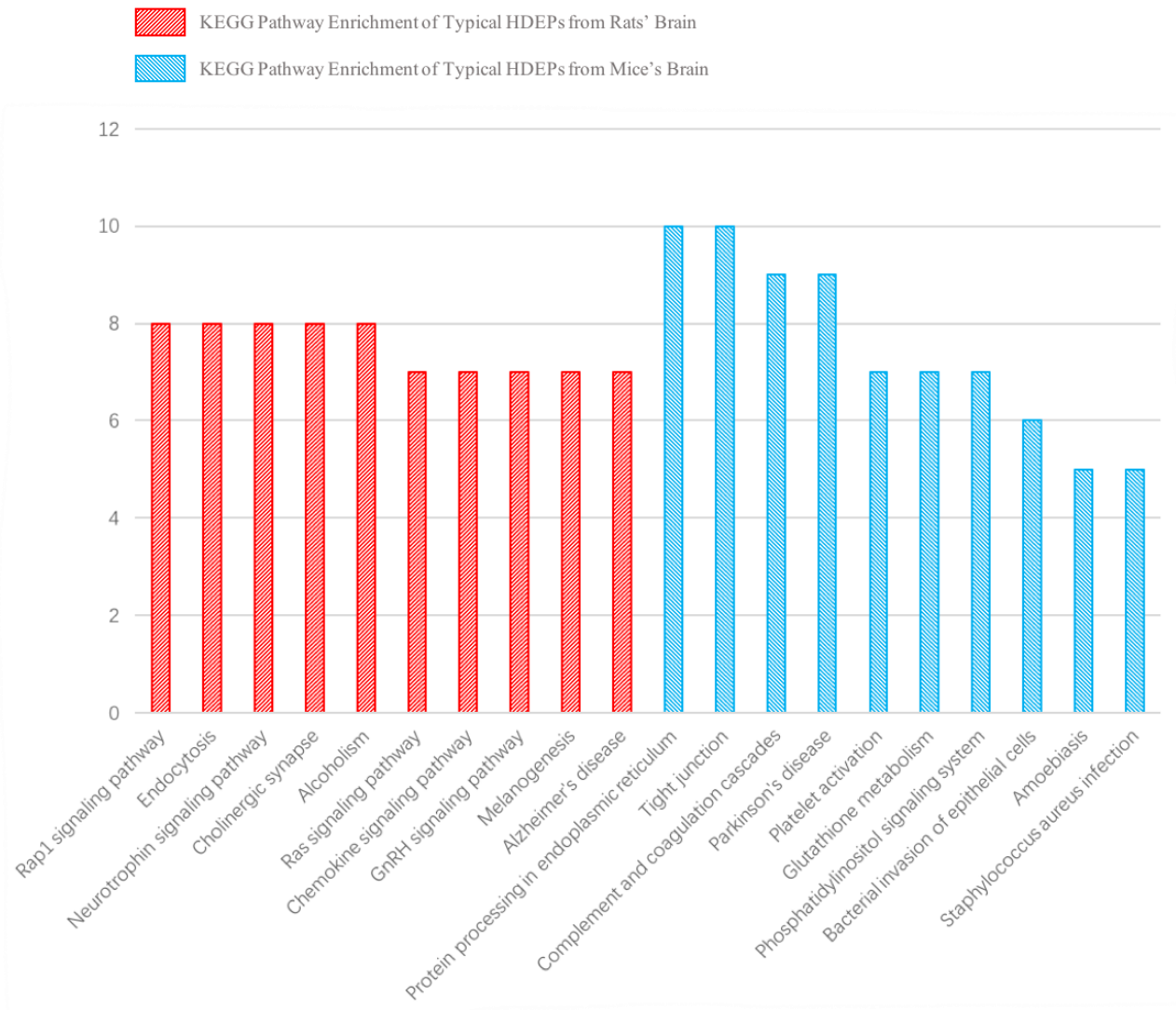


Fig. 4. The most enriched pathways of HDEPs. The clustered column shows the top 10 enriched pathways of typical HDEPs from KM mice and the other 10 of typical HDEPs from SD rats.

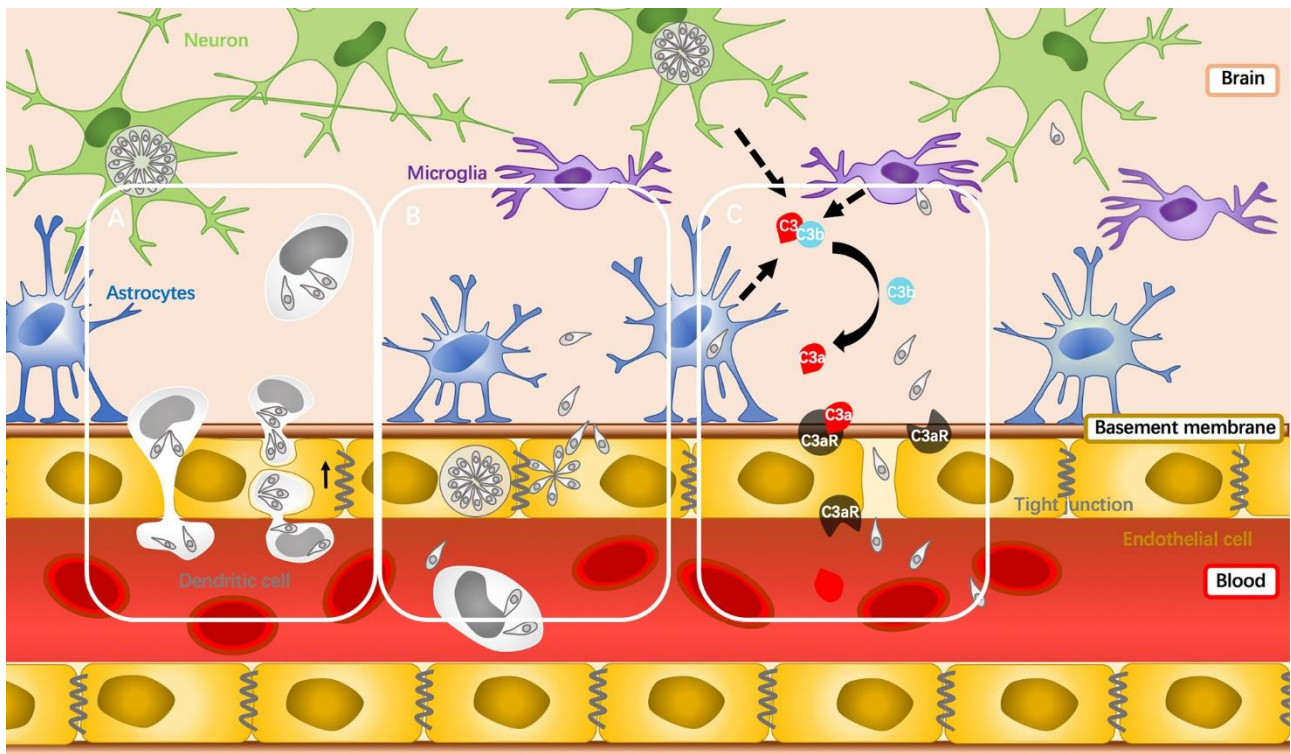


Fig. 5. The routes of *T. gondii*'s brain infection. (A) Trojan-horse like mechanism: The infected immune cells bring the intracellular parasites through the BBB. (B) Transcellular crossing mechanism: The bloodstream tachyzoites adhere to, invade in, replicate at, and pass from the endothelial cells of CNS to enter the CNS parenchyma. (C) Paracellular entry mechanism: Cooperating with C3 the bloodstream tachyzoites may directly cross the BBB through the brain TJ.